Supporting Information

Surface chemistry of passive films on Ni-free stainless steel: the effect of organic components in artificial saliva.

Deborah Biggio, Bernhard Elsener, Giulia Usai, Marzia Fantauzzi, *Antonella Rossi**

AUTHOR ADDRESS

Dipartimento di Scienze Chimiche e Geologiche, Università di Cagliari, Cittadella Universitaria, 09042, Monserrato, Cagliari, Italy

AUTHOR INFORMATION

Corresponding authors

Antonella Rossi - *Dipartimento di Scienze Chimiche e Geologiche, Università di Cagliari, Cittadella Universitaria, 09042, Monserrato, Cagliari, Italy*, antonella.rossi@unica.it.

Marzia Fantauzzi- *Dipartimento di Scienze Chimiche e Geologiche, Università di Cagliari, Cittadella Universitaria, 09042, Monserrato, Cagliari, Italy*, marzia.fantauzzi@unica.it

(M. Fantauzzi and A. Rossi are both corresponding author of this work.)

Authors

Deborah Biggio- *Dipartimento di Scienze Chimiche e Geologiche, Università di Cagliari, Cittadella Universitaria, 09042, Monserrato, Cagliari, Italy*

Bernhard Elsener- *Dipartimento di Scienze Chimiche e Geologiche, Università di Cagliari, Cittadella Universitaria, 09042, Monserrato, Cagliari, Italy*

Giulia Usai- *Dipartimento di Scienze Chimiche e Geologiche, Università di Cagliari, Cittadella Universitaria, 09042, Monserrato, Cagliari, Italy*

Table of Contents

Figures **14**

Tables

Table S1: bulk composition of the DIN 1.4456 stainless-steel was determined by X-ray fluorescence spectroscopy (XRF). Mean values over three independent measurements are provided, and standard deviations are given in parentheses. A hand-held standardless - XRF spectrometer, SPECTRO xSORT (Spectro Analytical Instruments GmbH, Kleve, Germany) was used. The instrument is equipped with a miniaturized X-ray Rh-anode and in these measurements an acceleration voltage of 50 kV was applied; the current was 10 μA and the acquisition time was 10 s.

Alloying elements	**Fe**	**Cr**	**Mn**	**Mo**	**Ni**	**C**	**S**	**Si**	**N**	**P**
Nominal wt %	60.1	17.9	18.4	1.9	0.18	0.06	0.04	0.9	0.8	0.025
XRF wt%	59 (1)	20 (1)	18.2 (0.1)	1.91 (0.05)	0.13 (0.03)					

Details on XRF measurements

This hand-held standardless SPECTRO xSORT (Spectro Analytical Instruments GmbH, Kleve, Germany) spectrometer allows obtaining the composition of metals and alloys, minerals and environmental samples including solutions. For each sample type, a proper set-up (filament current and acquiring time) is applied to record the spectra. A proper calibration algorithm based on the fundamental parameter is then automatically applied to obtain the concentration of the elements.

The fundamental parameters approach for the calibration relies on correcting the experimental areas for coefficients that consider both instrumental conditions, such as tube emissions and detector efficiency, and element–related factors, such as fluorescence intensities, absorption coefficients, absorption edges. In the present work a preset analysis method called “Precious metals” was used. For this method a current of 10 μA was applied and the acquisition time was 10 s. To assure accurate measurements of the energy and of peak intensity, a calibration is performed as often as required by the instrument, typically when it is turned on and periodically during long analysis session. The calibration is automatically performed by the instrument with the ICAL function that is part of the Spectro xSORT software. ICAL relies on measuring the intensity and the energy of Cr, Ni and Mo lines in an alloy constituting a shutter. During the calibration an acceleration voltage of 40 kV and a current of 9 μA were applied for 30 s. An algorithm then determines the current detector resolution, calculates the spectrum-energy-correlation and the X-ray intensity.

Table S2: Mechanical polishing procedure

Step	**Grinding**			**Polishing**		
Surface	500 SiC paper	1200 SiC paper	2400 SiC paper	DP Plus cloth with 3 mm diamond paste	DP Plus cloth with 1 mm diamond paste	DP Plus cloth with ¼ mm diamond paste

Lubricant	Bi-distilled water	Bi-distilled water	Bi-distilled water	Ethanol	Ethanol	Ethanol
Time [min.]	3	3	2	1.30	1	1

The samples were washed with bi-distilled water after each griding step, and with analytical-grade EtOH after each polishing step. After the last step, the samples were rinsed with EtOH in ultra-sonic bath for two minutes.

Table S3: Chemical composition (g / dm^3) of saliva solutions. Solutions' pH was measured when the solutions were made up; mean values were determined over three independent measurements and standard deviations are provided in parentheses in agreement with the guidelines published in Eurachem/CITAC guide: Quantifying Uncertainty in Analytical Measurement[2]. The composition of the Tani-Zucchi formulation is provided for comparison in the footnote ‡.

D*: pH = 6.9 (0.1)		**C-B: pH = 8.1 (0.2)**	**SALMO: pH = 8.30 (0.04)**
Stock A (g / dm^3)	Final concentration (g / dm^3)		0.52 NaCl
56 NaH_2PO_4		0.70 NaCl	0.58 KCl
150 NaCl	1.50 NaCl	1.20 KCl	0.23 $CaCl_2$
22 NH_4Cl	0.22 NH_4Cl	0.26 KH_2PO_4	0.10 $MgCl_2 \cdot 6H_2O$
2.2 $Na_3C_6H_5O_7 \cdot 2\ H_2O$	0.56 NaH_2PO_4	0.33 KSCN	0.19 K_2SO_4
7.0 lactic acid ($C_3H_6O_3$)	0.004 NaOH	0.19 Na_2HPO_4	0.00011 NaF
Stock B (g / dm^3)	0.60 $NaHCO_3$	1.50 $NaHCO_3$	0.96 $NaHCO_3$
10.0 urea (CH_4N_2O)	0.20 NaSCN	0.13 Urea (CH_4N_2O)	1.48 K_2HPO_4
0.75 Uric acid ($C_5H_4N_4O_3$)	0.022 $Na_3C_6H_5O_7 \cdot 2\ H_2O$		0.19 NH_4Cl
0.2 NaOH	0.07 lactic acid ($C_3H_6O_3$)		0.19 KSCN
Stock C (g / dm^3)	0.20 urea (CH_4N_2O)		0.03 Glycine ($C_2H_5NO_2$)
60.0 $NaHCO_3$	0.015 Uric acid ($C_5H_4N_4O_3$)		0.20 urea (CH_4N_2O)
20.0 NaSCN			

*Darvell solution was prepared by adding 10 cm^3 of stock A, 20 cm^3 of stock B and 10 cm^3 of stock C in 1 dm^3, following the procedure described in literature [3].

‡ Composition of Tani-Zucchi formulation [4]: $NaHCO_3$ 0.13 g / dm^3; KSCN 0.5 g / dm^3; KCl 1.5 g / dm^3; NaH_2PO_4 0.17 g / dm^3; urea (CH_4N_2O) 0.1 g / dm^3 ; α-amylase 0.1 mg / dm^3; pH = 7.9 (0.1)

Table S4. Polarization resistance (Rp) mean values ($M\Omega \cdot cm^2$) of stainless-steel DIN 1.4456 exposed to model solutions: D, pH= 6.9 (0.1), C-B pH= 8.1 (0.2), and SALMO pH= 8.30 (0.04)) for 1 h (Rp_{1h}), 3 h (Rp_{3h}) and 16 h (Rp_{16h}). Standard deviations are given in parentheses.

Model solutions	Rp_{1h} [$M\Omega \cdot cm^2$]	Rp_{3h} [$M\Omega \cdot cm^2$]	Rp_{16h} [$M\Omega \cdot cm^2$]
D	0.42 (0.06)	0.6 (0.1)	1.2 (0.1)
C-B	0.28 (0.09)	1.1 (0.2)	1.9 (0.6)
SALMO	0.38 (0.02)	0.6 (0.2)	1.2 (0.3)

Table S5: Binding energy values (eV), line shape: Gaussian/Lorentzian product functions - GL(x) (x = mixing factor) are given in this table; T is a tail function, and FWHM height is the full width at half-maximum height (eV) of the most intense iron, chromium, manganese, molybdenum, phosphorus, oxygen and calcium photoelectron peaks. Binding energy values are provided in the table as mean values. The standard deviations of the binding energy values are found to be equal to ± 0.1 eV in all cases. Line shapes, FWHM and mixing factors were determined on reference compounds and constrained for processing these spectra. All constraints are reported. Please, note that the column labelled FWHM lists the values that were set for curve-fitting the spectra; the following one gives the constraints applied for the fitting.

	MP BE (± 0.1 eV)	D BE (± 0.1 eV)	C-B BE (± 0.1 eV)	SALMO BE (± 0.1 eV)	Constraints				
					Line shape	Position (eV)	FWHM (± 0.1 eV)	FWHM (eV)	Area
Fe $2p_{3/2}$ – Fe (0)	707.0	706.9	706.9	706.9	GL(85)T(0.8)	/	1.04	0.9 - 1.1	
Fe $2p_{3/2}$ – Fe (II) oxide	709.7	709.5	709.5	709.5	GL(30)	Fe $2p_{3/2}$ -Fe (0) + 2.6	2.25	Fe $2p_{3/2}$ -Fe (0) * 2.15	
Fe 2p3/2 – Fe (II) oxide sat.	715.2	715.1	715.1	715.1	GL(30)	Fe $2p_{3/2}$ -Fe (0) + 8.2	2.35	Fe $2p_{3/2}$ -Fe (0) * 2.15	Fe $2p_{3/2}$ -Fe (II) oxide * 0.08
Fe $2p_{3/2}$ – Fe (III) oxide	710.9	710.8	710.8	710.8	GL(30)	Fe $2p_{3/2}$ -Fe (0) + 3.9	2.72	Fe $2p_{3/2}$ -Fe (0) * 2.6	
Fe $2p_{3/2}$ – Fe (III) oxy-hydroxide	712.4	712.3	712.3	712.3	GL(50)	Fe $2p_{3/2}$ -Fe (0) + 5.4	2.72	Fe $2p_{3/2}$ -Fe (0) * 2.6	
Fe $2p_{3/2}$ – Fe (III) phosphate	-	713.8	713.8	713.8	GL(50)	713.8	3.70	Fe $2p_{3/2}$ -Fe (0) * 4.5	
Cr $2p_{3/2}$ – Cr (0)	574.0	574.0	574.0	574.0	GL(65)T(1)	/	1.0	1.3-1.5	
Cr $2p_{3/2}$ – Cr (III) oxide	576.5	576.5	576.5	576.5	GL(30)	Cr $2p_{3/2}$ – Cr (0) + 2.5	2.3	Cr $2p_{3/2}$ – Cr (0) * 2.3	
Cr $2p_{3/2}$ – Cr (III) hydroxide	577.2	577.1	577.1	577.1	GL(30)	Cr $2p_{3/2}$ – Cr (0) + 3.1	2.8	Cr $2p_{3/2}$ – Cr (0) * 2.8	
Cr $2p_{3/2}$ – Cr (III) phosphate		578.1	578.1	578.1	GL(30)	Cr $2p_{3/2}$ – Cr (0) + 4.1	2.3	Cr $2p_{3/2}$ – Cr (0) * 2.3	
Mn $2p_{3/2}$ – Mn (0)	638.7	638.6	638.6	638.6	GL(80)T(0.55)	/	1.0	0.8-1.0	
Mn $2p_{3/2}$ – Mn (III) oxi-hydroxide	640.9	641.0	641.0	641.0	GL(90)	Mn $2p_{3/2}$ - Mn (0) + 2.4	2.1	0-3	
Mn $2p_{3/2}$ -Mn (IV) oxide	642.5	642.3	642.3	642.3	GL(90)	Mn $2p_{3/2}$ - Mn (0) + 3.7	2.1	Mn $2p_{3/2}$ - Mn (III) *1	
Mo $3d_{5/2}$ – Mo (0)	227.9	227.8	227.8	227.8	GL(60)T(1.2)	/	1.4	1.3-1.5	
Mo $3d_{5/2}$ – Mo (IV) oxide	231	230.9	230.9	230.9	GL(45)	Mo$3d_{5/2}$- Mo (0) + 3.1	3.2	Mo$3d_{5/2}$- Mo (0) * 2.3	
Mo $3d_{5/2}$ – Mo (VI) oxide	232.4	232.3	232.3	232.3	GL(45)	Mo$3d_{5/2}$- Mo (0) + 4.8	2.0	Mo$3d_{5/2}$- Mo (0) * 1.4	
Mo $3d_{3/2}$ – Mo (0)	227.9	227.8	227.8	227.8	GL(60)T(1.2)	Mo$3d_{5/2}$- Mo (0) + 3.15	1.4	Mo$3d_{5/2}$- Mo (0) * 1	Mo$3d_{5/2}$- Mo(0) * 0.67

Mo $3d_{3/2}$ – Mo (IV) oxide	231	230.9	230.9	230.9	GL(45)	$Mo3d_{5/2}$- Mo (0) + 6.25	3.2	$Mo3d_{5/2}$- Mo (0) * 2.3	$Mo3d_{5/2}$-Mo (IV) * 0.67
Mo $3d_{3/2}$ – Mo (VI) oxide	232.4	232.3	232.3	232.3	GL(45)	$Mo3d_{5/2}$- Mo (0) + 7.95	2.0	$Mo3d_{5/2}$- Mo (0) * 1.4	$Mo3d_{5/2}$- Mo (VI) 0.67
O 1s – oxide	530.3	530.4	530.3	530.3	GL(30)	/	1.4	1.3-1.5	
O 1s – hydroxide	531.9	531.8	531.7	531.7	GL(30)	/	1.4	O (oxide) *1	
O 1s – adsorbed H_2O	533.0	533.1	533.0	533.1	GL(30)	/	1.4	O (oxide) *1	
P $2p_{3/2}$ phosphate**	-	133.5	133.5	133.5	GL(30)	/	1.4	/	
P $2p_{1/2}$ phosphate	-	134.4	134.4	134.4	GL(30)	P $2p_{3/2}$ + 0.87	1.4	P $2p_{3/2}$ *1	P $2p_{3/2}$ *0.5
Ca $2p_{3/2}$ phosphate	-	-	-	347.8	GL(30)	/	1.6	/	
Ca $2p_{1/2}$ phosphate	-	-	-	351.3		Ca $2p_{3/2}$ + 3.5	1.6	Ca $2p_{3/2}$ *1	Ca $2p_{3/2}$ *0.5
C 1s - aliph.	285.0	285.0	285.0	285.0	GL(30)	/	1.5	1.4-1.6	
C 1s – C-O	286.7	286.7	286.7	286.7	GL(30)	/	1.5	C -aliph *1	
C 1s – C=O	288.7	288.7	288.7	288.7	GL(30)	/	1.5	C -aliph *1	

Curve fitting was carried out using CASA XPS software version 2.3.24PR1.0
*The BE value of the P 2p peak maximum (centroid) is at 133.6 eV

Table S6. v_{corr} and weight loss calculated for the Ni-free DIN 1.4456 stainless steel exposed D pH= 6.9 (0.1), C-B pH= 8.1 (0.2), and SALMO pH= 8.30 (0.04) for 16 hours. The data of T-Z pH= 7.9 (0.1)after 24 hours from [1] are reported for comparison. From the i_{corr} ($\mu A/cm^2$) values, the corrosion rate v_{corr} (μm/year) were calculated by applying the Faraday law (conversion factor to calculate v_{corr} from i_{corr} is 1 $\mu A/cm^2$ = 11.7 μm/year)

	v_{corr} (μm/year)	Weight loss (μg/cm²week)
DARVELL	0.52 (0.06)	6.2 (0.7)
C-B	0.3 (0.1)	4 (2)
SALMO	0.5 (0.2)	6 (2)
Tani-Zucchi (24 h)	0.23 (0.02)	2.8 (0.3)

Table S7. Stability constants of ML complexes. Data from literature. [5-10]

M^{n+}	Ligands				
	Urea	SCN^-	citrate	Uric acid	Lactic acid
	Stability constant: $Log\beta_1$				
Fe^{3+}	/	2.94 [5]	13.3 [6]	11.04 [7]	7.1[8]
Cr^{3+}	/	2.52[5]	7.69 [9]	/	3.3 [10]

Figures

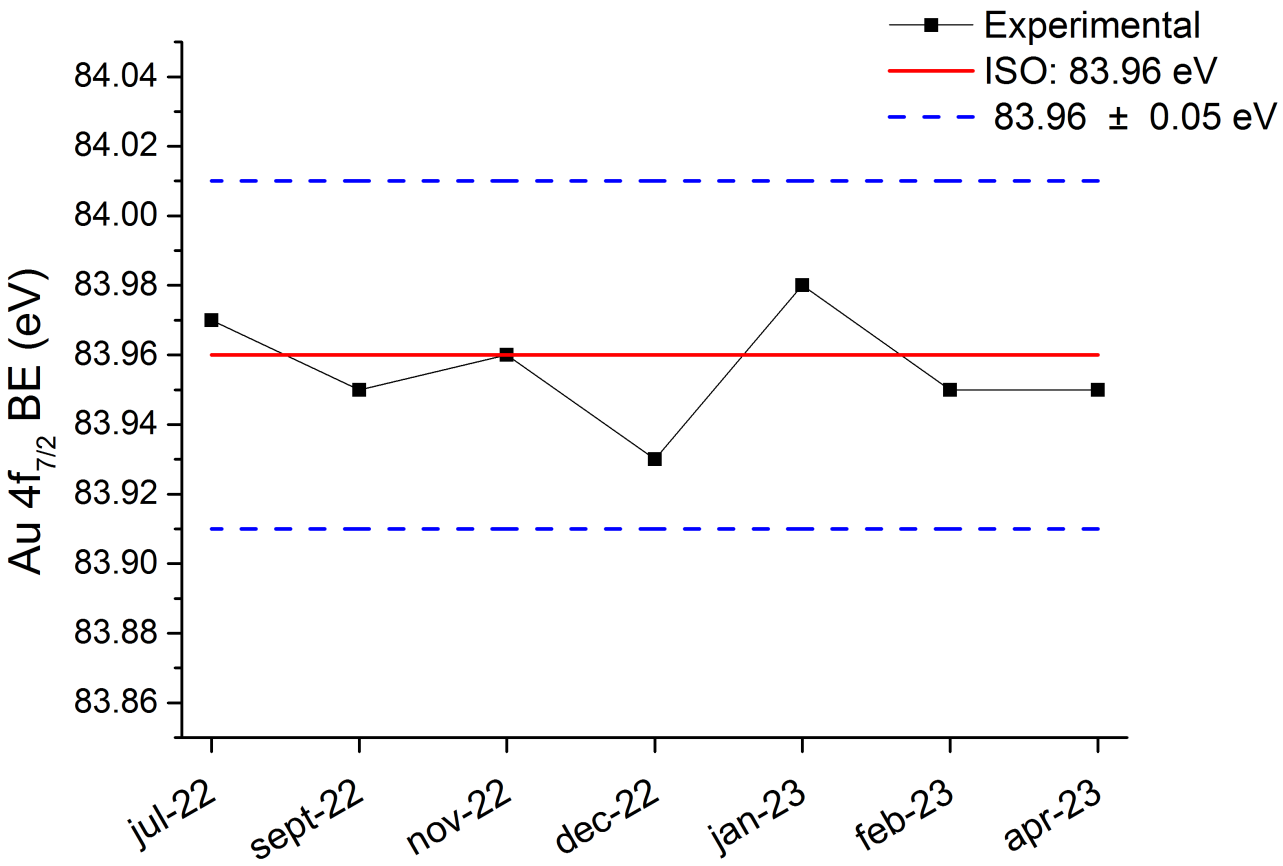

Figure S1: Au $4f_{7/2}$ binding energy control chart. The control line refers to the binding energy reported in ISO 15472:2010 for a sputter clean gold sample acquired with a monochromatic Al ka X-ray source (83.96 eV) and the upper and lower limit lines to 83.96 ± 0.05 eV.

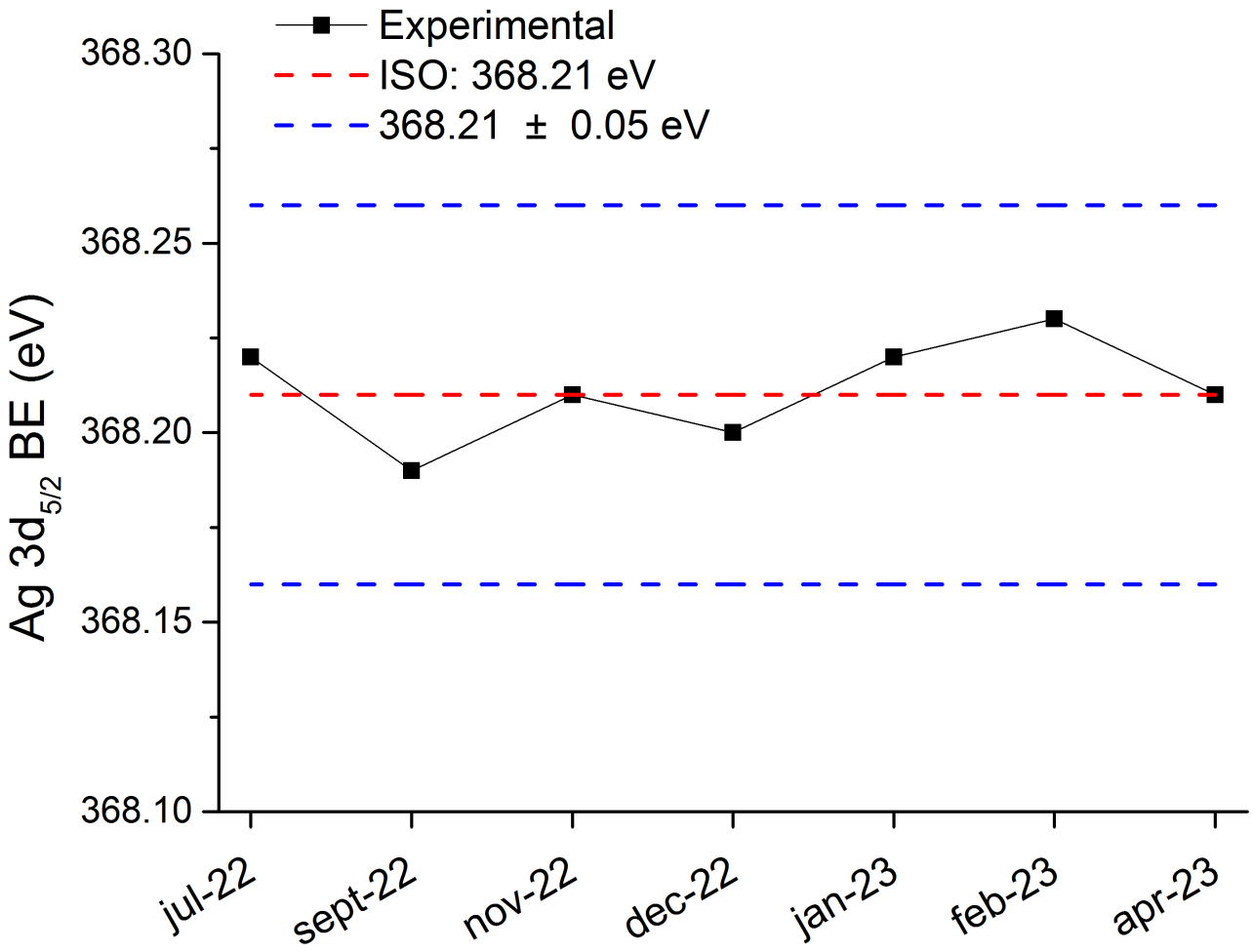

Figure S2: Ag $3d_{5/2}$ binding energy control chart. The control line refers to the binding energy reported in ISO 15472:2010 for a sputter clean silver sample acquired with a monochromatic Al ka X-ray source (368.21 eV) and the upper and lower limit lines to 368.21 ± 0.05 eV.

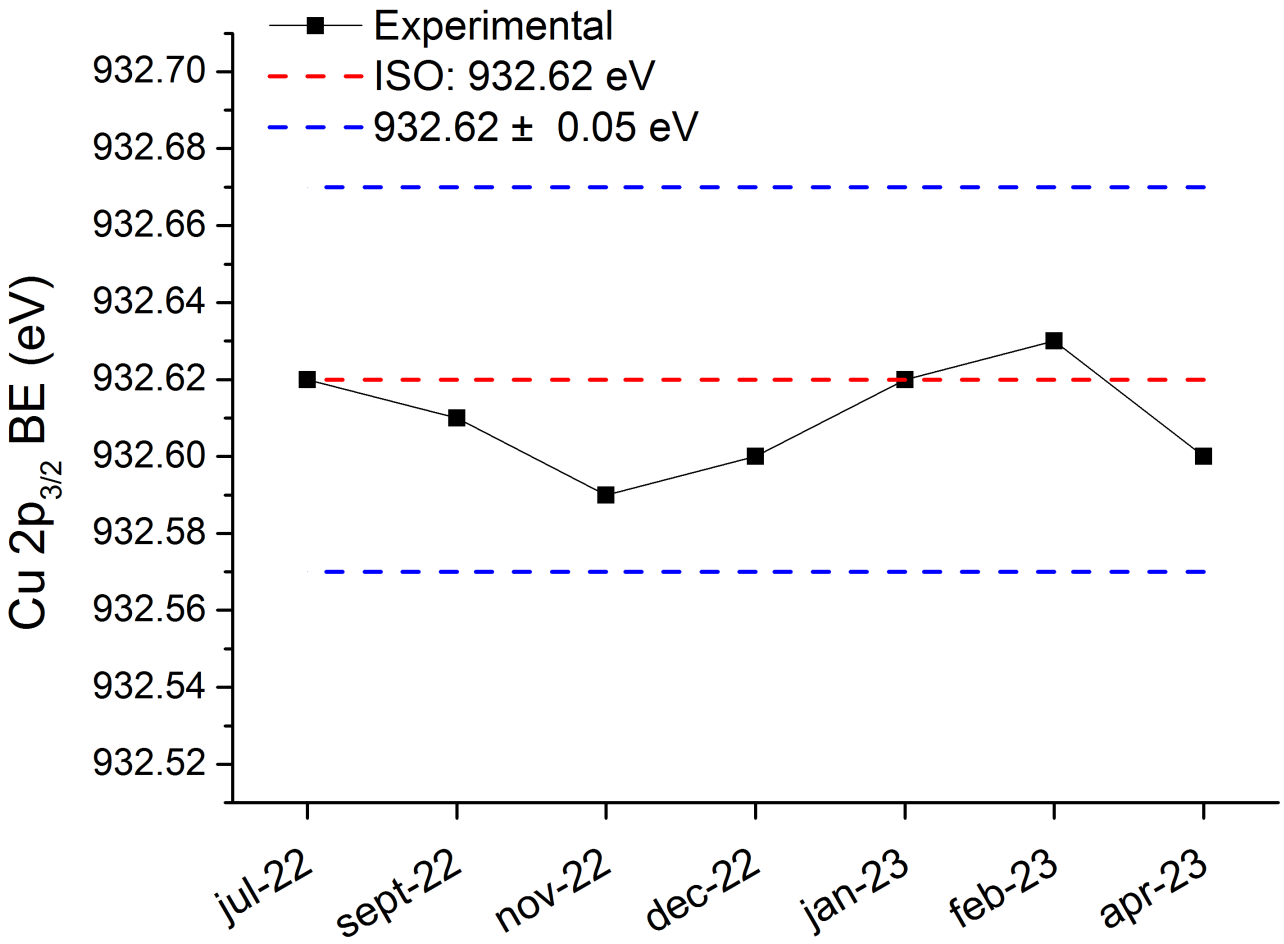

Figure S3: Cu $2p_{3/2}$ binding energy control chart. The control line refers to the binding energy reported in ISO 15472:2010 for a sputter clean copper sample acquired with a monochromatic Al ka X-ray source (932.62 eV) and the upper and lower limit lines to 932.62± 0.05 eV.

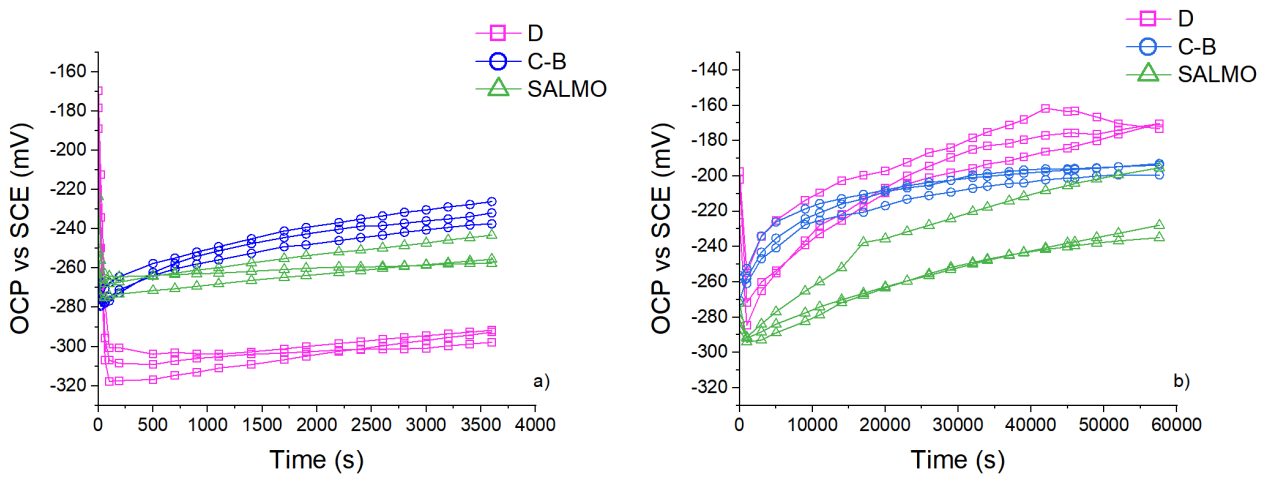

Figure S4: Open circuit potential versus time curves for mechanically polished stainless-steel DIN 1.4456 exposed for 1 h (a) and 16 h (b) to Darvell (D, pH= 6.9 (0.1) (magenta curves), Carter-Brugirard (C-B, pH= 8.1 (0.2)) (blue curves) and SALMO pH= 8.30 (0.04) (green curves) solutions. Three independent measurements for each solution were performed and in this picture all measurements are shown.

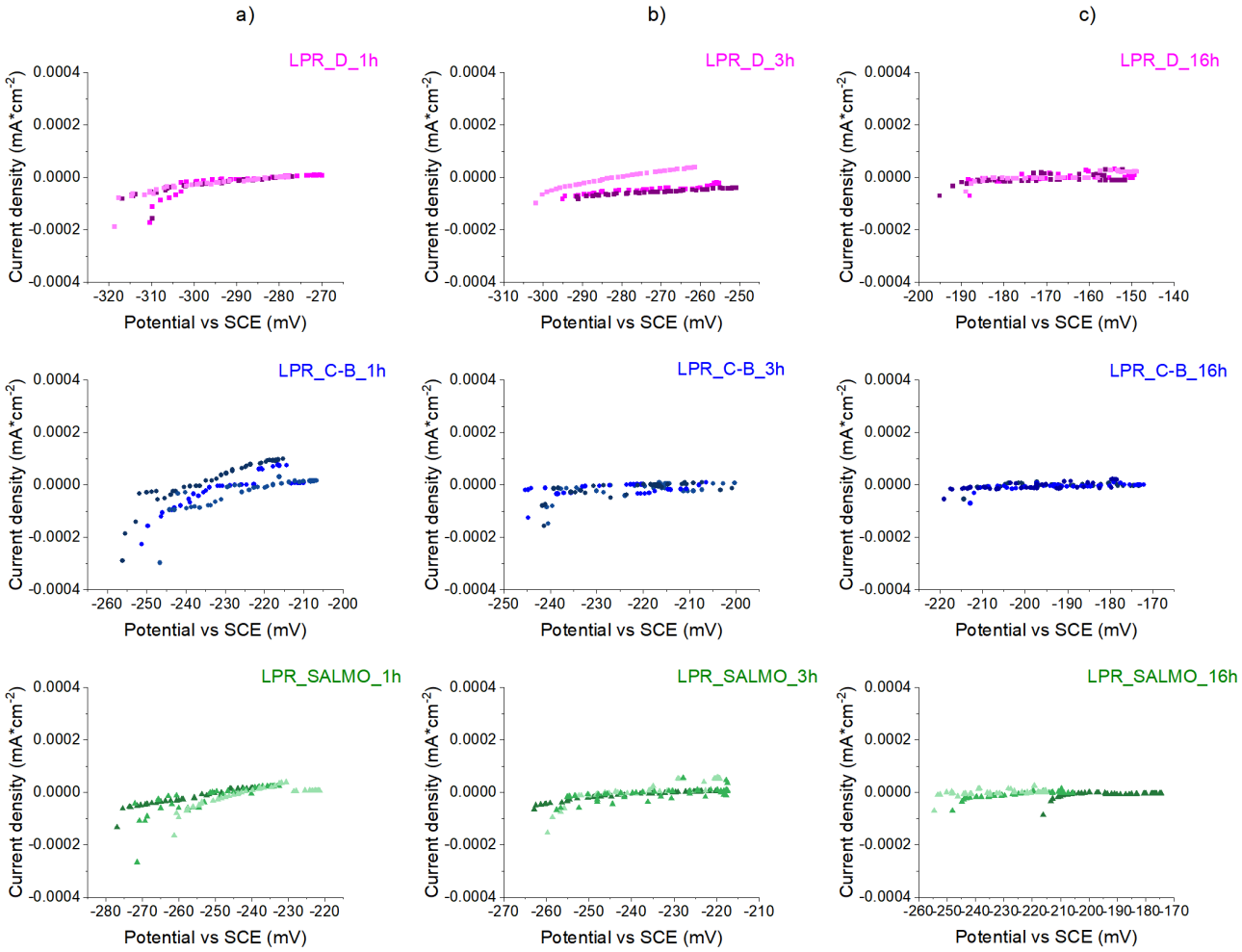

Figure S5: LPR plots current density (mA cm^{-2} vs potential vs SCE mV) of DIN 1.4456 stainless steel after: a) 1 h of exposure from top to down D (pH= 6.9 (0.1)), C-B (pH= 8.1 (0.2)), and SALMO (pH= 8.30 (0.04)); b) 3 h of exposure from top to down D; C-B; SALMO; c) 16 h of exposure from top to down D; C-B; SALMO.

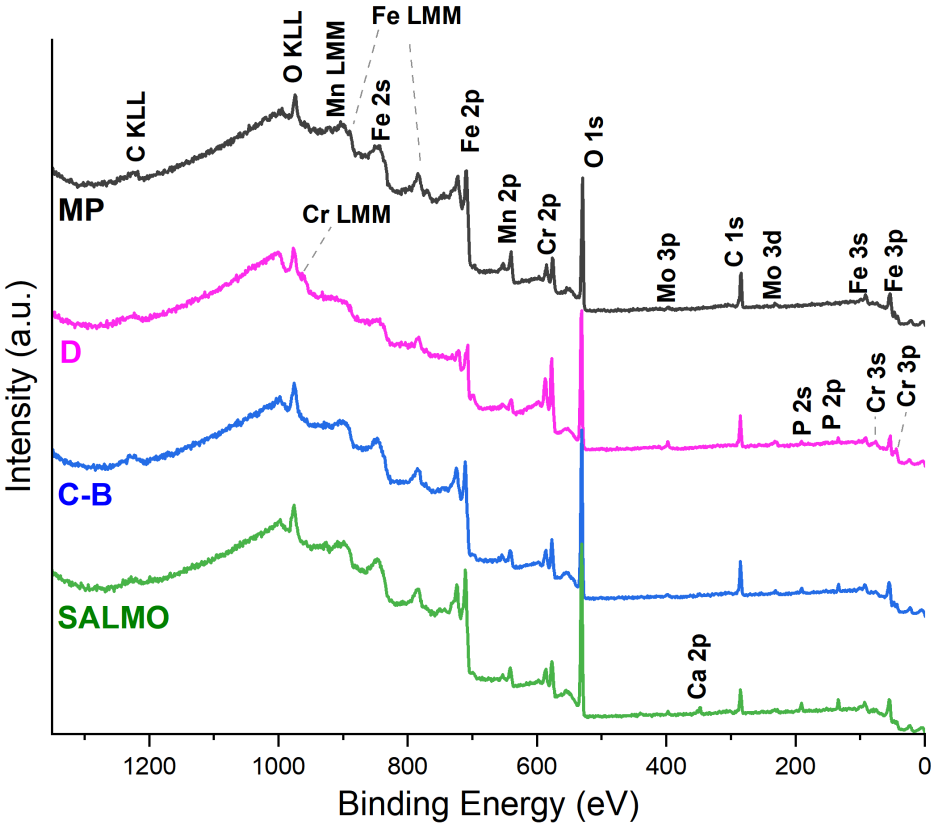

Figure S6. Survey spectra of Ni-free DIN 1.4456 stainless steel after mechanical polishing (MP) and after exposure for one hour of exposure to D pH= 6.9 (0.1), C-B pH= 8.1 (0.2), and SALMO pH= 8.30 (0.04) solutions. X-ray source: monochromatic Al kα operated at 6.7 mA and 15kV (100 W), 400µm spot size.

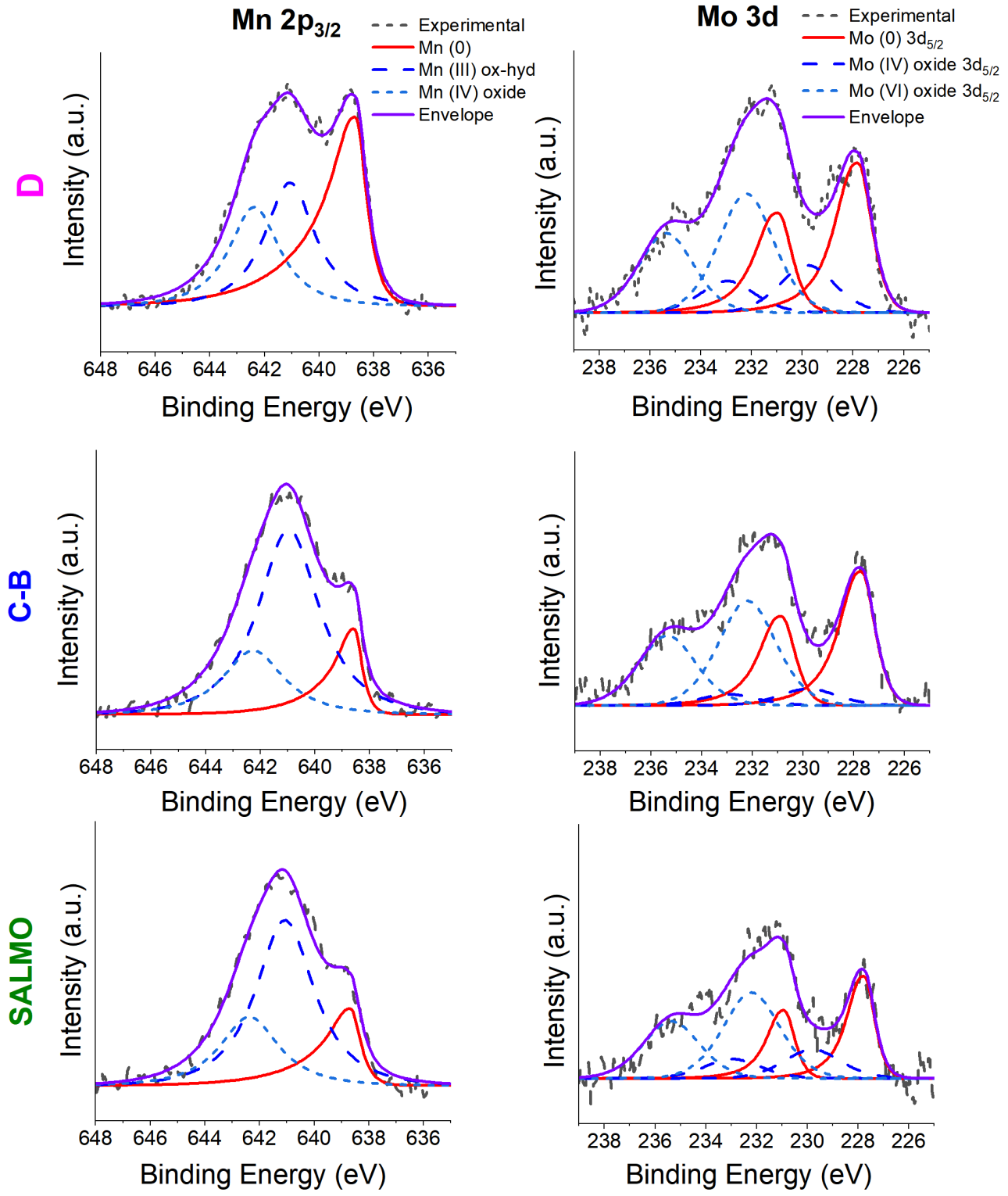

Figure S7: Mn $2p_{3/2}$ and Mo 3d signals of the DIN 1.4456 stainless steel exposed to D (pH= 6.9 (0.1)), C-B (pH= 8.1 (0.2)), and SALMO (pH= 8.30 (0.04)) formulations for 1h at the OCP.

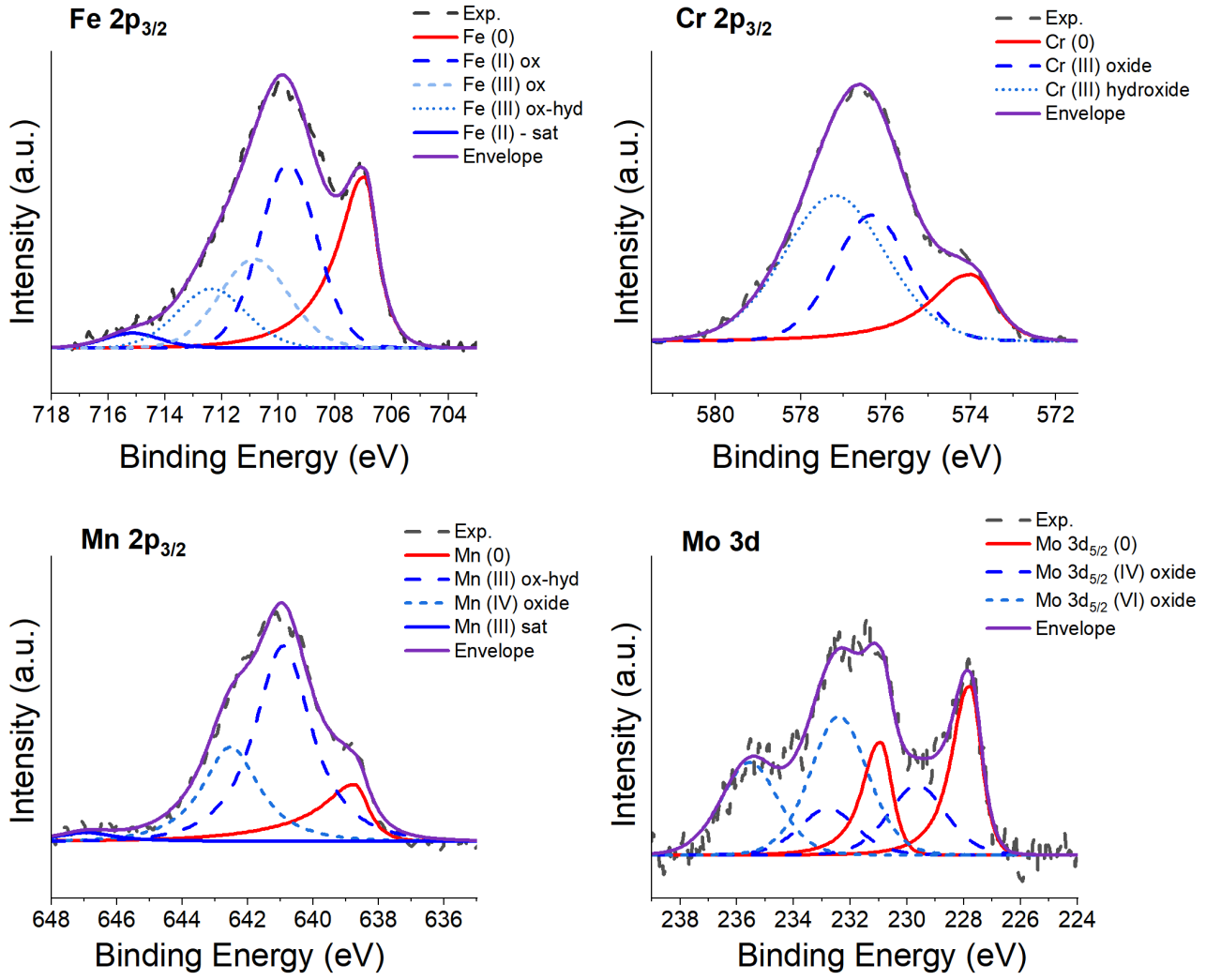

Figure S8: Fe $2p_{3/2}$, Cr $2p_{3/2}$,Mn $2p_{3/2}$ and Mo 3d signals of the mechanically polished DIN 1.4456 stainless steel.

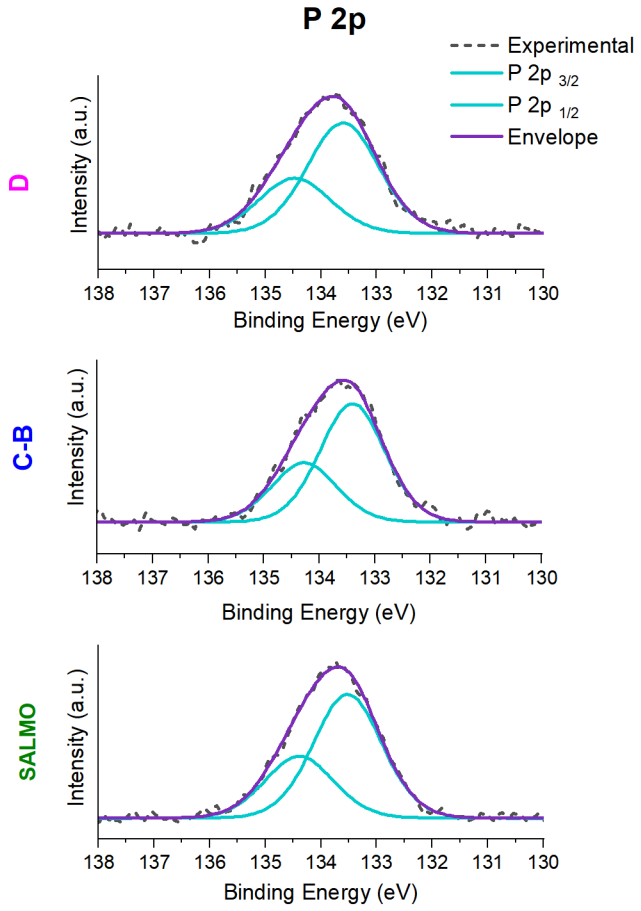

Figure S9: P 2p signals of the DIN 1.4456 stainless steel exposed to D (pH= 6.9 (0.1)), C-B (pH= 8.1 (0.2)), and SALMO (pH= 8.30 (0.04)) formulations for 1h at the OCP.

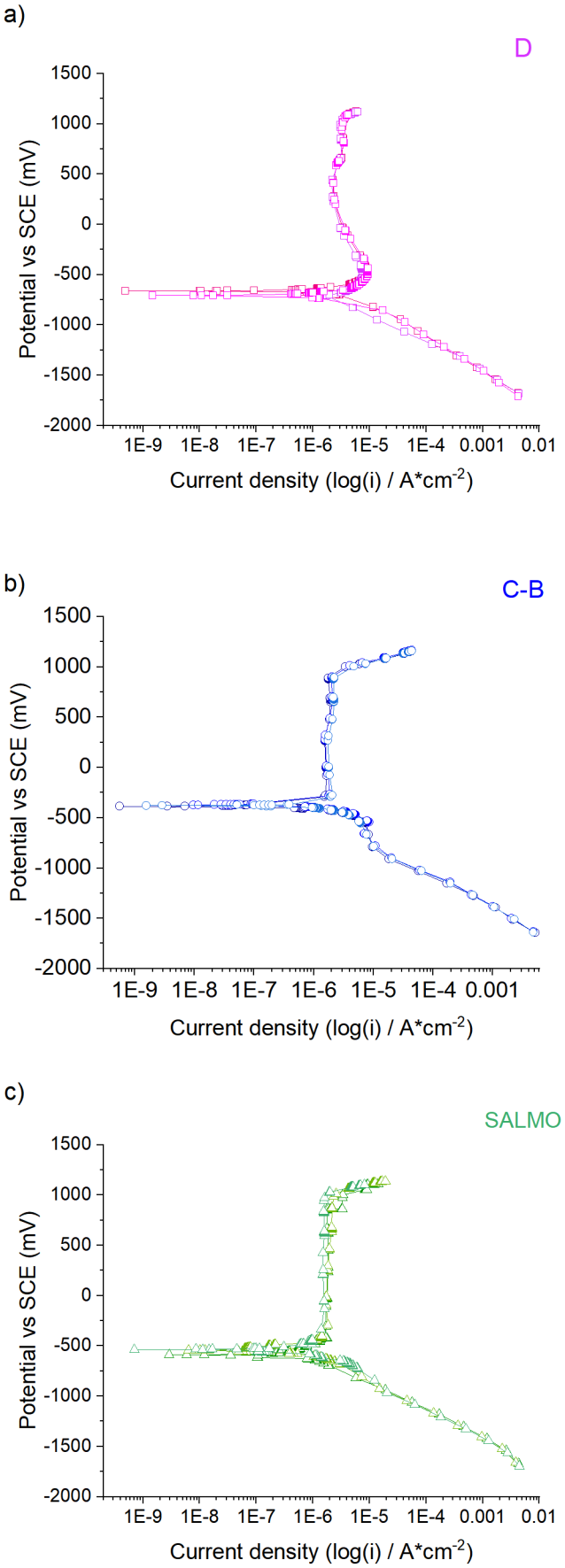

Figure S10: Potentiodynamic polarization curves of stainless-steel DIN 1.4456 after 1 h of contact with a) Darvell D (pH= 6.9 (0.1)), b) C-B (pH= 8.1 (0.2)), and c) SALMO (pH= 8.30 (0.04)), artificial saliva solution. Three independent measurements for each solution were performed.

References

(1) Pisu, M. Stability of Dental Alloys in Artificial Saliva: An Electrochemical and XPS Investigation, University of Cagliari, **2013**.

(2) Ellison, S. L. R.; Williams, A. *Quantifying Uncertainty in Analytical Measurement, Third Edition*; Eurachem/CITAC guide; guide; **2012**.

(3) Darvell, B. W. The Development of an Artificial Saliva for in Vitro Amalgam Corrosion Studies. *J. of Oral Rehab.* **1978**, 41–49.

(4) Tani, G.; Zucchi, F. Electrochemical Valuation of the Corrosion Resistance of Commonly Used Metals in Dental Prosthesis. *Minerva Stomatologica*. 1967, 710–713.

(5) Bahta, A.; Parker, G. A.; Tuck, D. G. Critical Survey of Stability Constants of Complexes of Thiocyanate Ion (Technical Report). *Pure and Applied Chemistry* **1997**, *69* (7), 1489–1548. https://doi.org/10.1351/pac199769071489.

(6) Field, T. B.; McCourt, J. L.; McBryde, W. A. E. Composition and Stability of Iron and Copper Citrate Complexes in Aqueous Solution. *Can. J. Chem.* **1974**, *52* (17), 3119–3124. https://doi.org/10.1139/v74-458.

(7) Davies, K. J.; Sevanian, A.; Muakkassah-Kelly, S. F.; Hochstein, P. Uric Acid-Iron Ion Complexes. A New Aspect of the Antioxidant Functions of Uric Acid. *The Biochemical journal* **1986**, *235* (3), 747–754.

(8) Martell, A. E. *Stability Constants of Metal-Ion Complexes*, 2nd edition.; Eds. London: The chemical society, **1964**.

(9) Vinokurov, E. G.; Bondar', V. V. Prediction of Stability Constants for Cr(III) and Cr(II) Complexes. *Russian Journal of Coordination Chemistry* **2003**, *29* (1), 66–72. https://doi.org/10.1023/A:1021851219309.

(10) Portanova, R.; Lajunen, L. H. J.; Tolazzi, M.; Piispanen, J. Critical Evaluation of Stability Constants for Alpha-Hydroxycarboxylic Acid Complexes with Protons and Metal Ions and the Accompanying Enthalpy Changes. Part II. Aliphatic 2-Hydroxycarboxylic Acids (IUPAC Technical Report). *Pure and Applied Chemistry* **2003**, *75* (4), 495–540. https://doi.org/10.1351/pac200375040495.